

Distributed fiber temperature alarm system based on thermodynamic phase transition

Li Zhang, Fan Yang*, Flavien Gyger, and Luc Thévenaz

Swiss Federal Institute of Technology Lausanne (EPFL), Group for Fibre Optics,
SCI-STI-LT Station 11, 1015 Lausanne, Switzerland

*Corresponding author: fan.yang@epfl.ch

Abstract: A novel temperature sensing mechanism is proposed for the first time, based on thermodynamic phase transitions of CO₂ in hollow-core fibers. A fast, sensitive and distributed fiber temperature alarm system is demonstrated using this concept. © 2021 The Author(s)

1. Introduction

Optical fibers enable unique possibility of performing distributed sensing over long sensing lengths. Such sensors show electromagnetic immunity, intrinsic safety, small size and weight, capability of remote detection. They have diverse important applications.

Distributed temperature sensing based on Brillouin optical correlation-domain analyzer has been demonstrated in gas-filled hollow-core photonic crystal fibers [1]. However, such systems are of high complexity and require a scanning procedure along the whole fiber length, which considerably slows down their response time.

Here, we propose a novel temperature sensing concept applicable for distributed temperature alarm detection, based on thermodynamic phase transitions of CO₂ filled in hollow-core photonic crystal fibers (HC-PCFs). When the temperature locally drops below the liquefaction point of gaseous CO₂, the gas condensates, inducing a sudden loss of guidance and a reflection of the interrogating light. The distributed temperature alarm shows a response time of the order of one second and ultra high sensitivity. The preset alarm temperature can be conveniently adjusted by changing the gas pressure in the HC-PCF.

2. Working principle

The phase of a thermodynamic system depends on its temperature and pressure. As a result, the temperature/pressure diagram is of discrete domains delimiting the different phases of the substance. A gaseous substance can undergo a gas-to-liquid phase transition when its temperature drops below a certain critical temperature T_c , at a constant pressure. Opposite transition occurs when the temperature increases above T_c . For example, at 48 bar pressure, T_c of CO₂ is 13.85 °C, so CO₂ switches between gas and liquid phases if the environmental temperature crosses 13.85 °C. For each phase of the substance, the optical properties are very different, which can be used for sensing. So far, no sensing application taking advantage of a gas-liquid phase transition has been reported.

The working principle is illustrated in Fig. 1. CO₂ gas is filled into a 50-m-long HC-PCF (HC-1550-02 from NKT Photonics). Light is confined in the HC-PCF by the bandgap effect with a transmission band from 1500 to 1650 nm. Our operating wavelength (1550 nm) is located far away from any CO₂ absorption lines, so the system's insertion loss solely includes the HC-PCF attenuation (16 dB/km) and the coupling losses. CO₂ remains in its gas phase as long as the environmental temperature remains above T_c . This can be characterized as the *normal* state of the system. However, once the local temperature at a certain location drops below T_c (at t_1 in Fig. 1), the gas condensates in the HC-PCF, which induces a large attenuation in the C band. This is because the liquid CO₂ has a refractive index of ~ 1.2 (as compared to about 1.0 for the gaseous state), locally shifting the fiber's bandgap to a lower wavelength range (~ 800 nm) [2], thus resulting in a *high loss* at this fiber position and triggering an *alarm*. The system naturally returns to its *normal* state when the temperature returns back to a value above T_c (at t_2 in Fig. 1).

The alarm temperature defined by T_c , depends on the gas type and the internal pressure, which gives the system good reconfigurability. For example, for CO₂, the alarm temperature can be tuned from -50 °C to 30 °C by varying the pressure from 6 bar to 73 bar.

3. Experimental results

The structure of the alarm system is extremely simple, consisting of only three components, as shown in Fig. 1(a): a light source (e.g. light-emitting diode), a gas-filled HC-PCF and a photodetector at the output. In this study,

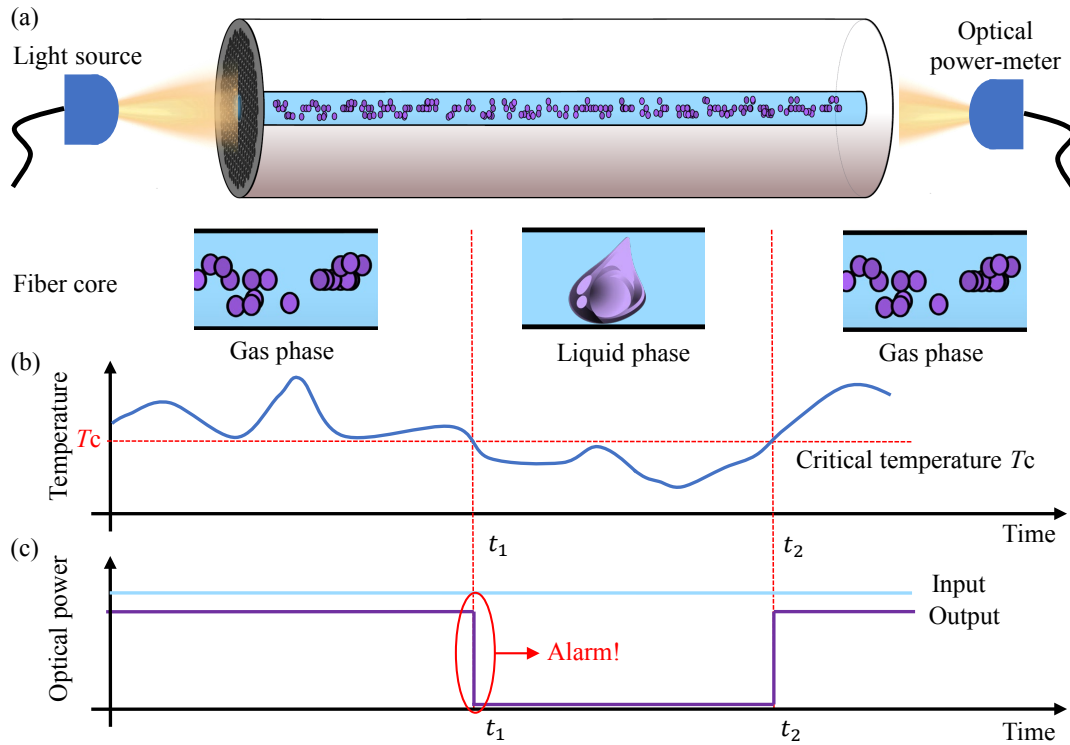


Fig. 1: Illustration of the working principle of the temperature alarm. (a) Systematic working setup. (b) Temperature variation as a function of time at an arbitrary location along the sensing fiber. (c) Optical power at the input and output of the sensing fiber.

we additionally use an ordinary optical time-domain reflectometry (OTDR) system in order to locate the position where the temperature dropped below T_c and triggered the alarm. The setup of the system is depicted in Fig. 2(a): an optical pulse is sent into the HC-PCF through a circulator and the time-dependent back-scattered light is collected by a photodetector. The electrical signal is then digitized by a 4 GHz bandwidth oscilloscope. The width of the interrogating optical pulse is set to 500 ps, which results in a spatial resolution of 7.5 cm. An optical power meter is inserted at the end of the fiber to monitor the transmission output and to trigger the alarm.

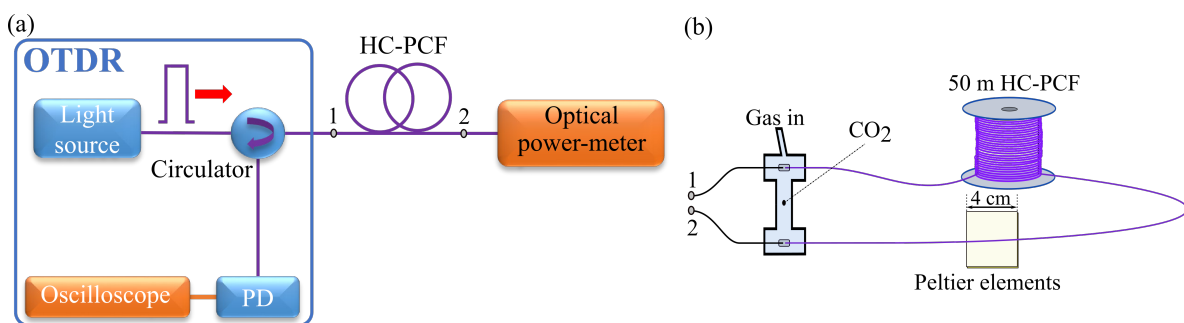


Fig. 2: (a) Systematic experimental setup implementing an optical time-domain reflectometer (OTDR). PD, photodetector. (b) Light and gas coupling to the HC-PCF and temperature test bench including two 4-cm-long Peltier elements. Black lines represent standard fiber patchcords while purple lines in (b) illustrate the HC-PCF.

The sensing fiber configuration and test bench is shown in Fig. 2(b). The CO_2 is filled in the HC-PCF via metal tubes and is externally maintained at a constant pressure. The HC-PCF gas cell is compact, robust and convenient to move as well as flexible to change the gas pressure inside. The detailed fabrication process can be found in [1]. At 0.9 m away from the far end of the HC-PCF, a 4-cm-long fiber section is placed between two Peltier elements, so that the temperature of this fiber section can be precisely controlled and monitored in real time.

3.1. Critical temperature

Firstly, the CO₂ critical temperature under different pressures is measured by monitoring the transmission of the fiber. The measured optical output power (normalized with peak output power), at a temperature around 13.9 °C and pressure of 48 bar, is shown in Fig. 3(a). Sharp changes take place when the temperature drops to 13.85 °C, which is consequently defined as the alarm temperature for 48 bar pressure. It should be noted that, a temperature change as small as 0.15 °C (between 14.00 °C and 13.85 °C) causes a huge change of the transmission loss (more than 60 dB), which demonstrates the ultra high sensitivity of this method. The response time shown in Fig. 3(a) is measured to be 1.5s, which includes the time required for the thermal change to reach the fiber core and the thermodynamic phase transition process to take place.

Secondly, T_c is characterized by our system as a function of the CO₂ pressure and the result is shown in Fig. 3(b). The measured critical temperatures lie slightly above the CO₂ liquid-gas phase transition curve (red curve in Fig. 3(b)) [3]. This is because the low-energy molecules of the Boltzmann distribution condense at slightly higher temperatures than the actual transition temperature (which corresponds to the average molecule energy). The good matching between the experimentally measured critical temperatures and the phase diagram demonstrates the reliability and reconfigurability of our method.

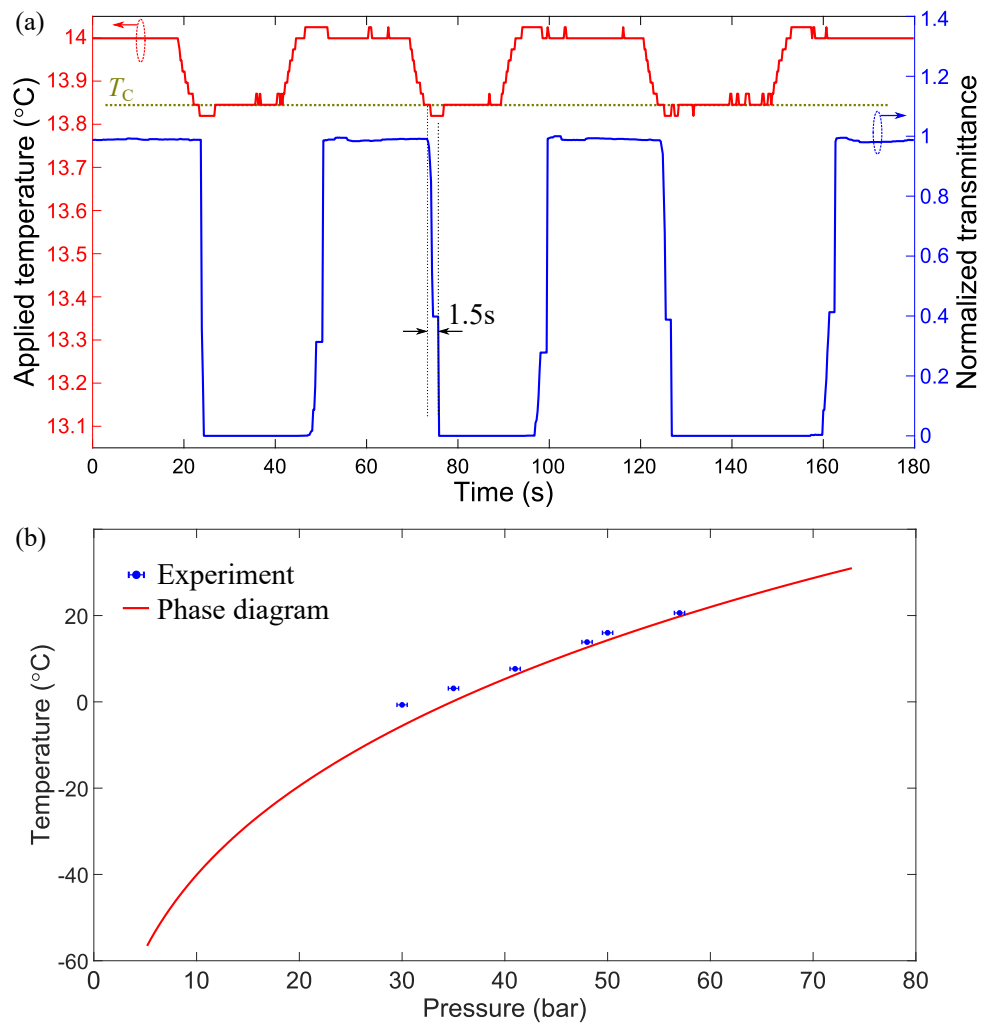


Fig. 3: (a) Measured optical output (blue line) as a function of the measured temperature at the fiber surface (red line). The HC-PCF is filled with 48 bar CO₂, corresponding to a critical temperature $T_c = 13.85$ °C. Alarms are reported each time the temperature drops from 14.00 °C to 13.85 °C, which demonstrates the ultra-high sensitivity of this sensing mechanism. (b) Measured critical temperature as a function of the CO₂ pressure (blue dots) as well as the phase diagram (red curve) [3]. The error bar in X axis is due to the pressure uncertainty of our pressure-meter.

3.2. Alarm point location

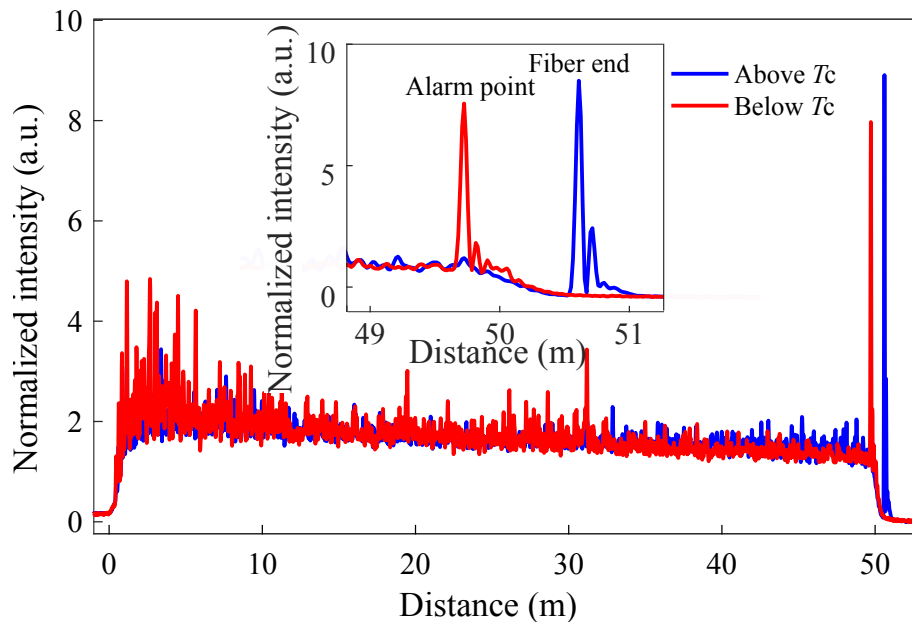


Fig. 4: OTDR traces when the alarm is off (blue trace) and on (red trace) at the test-bench position (alarm point). Inset: magnified trace between the alarm point and the fiber end.

An OTDR system is set up to precisely locate the alarm position along the fiber. The back-scattered traces of the fiber for a preset temperature below and above T_c are shown in Fig. 4 (with 100-times average). We can distinguish the position of the real fiber end, which appears as a peak on the blue line at around 50.7 m. When the temperature drops below T_c , the reflection from the fiber end disappears and a new reflection arises at around 49.8 m, as shown on the red trace in Fig. 4. This is because the refractive index of liquid CO_2 is around 1.2, which is larger than that of the gaseous CO_2 and causes a high reflection.

Clearly, the current alarm system is not able to report more than one alarm position simultaneously occurring along the sensing fiber because of the extremely high loss induced by the phase transition in the bandgap guiding HC-PCF. Nevertheless, a fully distributed temperature alarm system can be easily conceived by using a single-ring anti-resonant hollow-core fiber [4], which shows much smaller loss when the gas (refractive index of 1.0) changes to liquid state (refractive index of ~ 1.2). In this case, the gas to liquid phase transition brings measurable back-scattered light as well as tiny optical loss which can be detected by a simple OTDR.

4. Conclusion

A novel fiber sensing mechanism is proposed for the first time, based on the loss of guiding induced by a gas-liquid phase transition in the HC-PCF. Using this mechanism, a novel temperature alarm system is demonstrated by using only a light source, a power-meter and a compact HC-PCF gas cell. It shows ultra-high sensitivity (more than 60 dB transmission loss for less than 0.15°C temperature change), fast response time (1.5 s), reconfigurability and tunability of the transition temperature. In addition, the precise location of the alarm point is successfully resolved using a simple OTDR.

Acknowledgement

The European Union's Horizon 2020 research and innovation programme under the Marie Skłodowska-Curie grant agreement no. 722509 "FINESSE" and the SNSF under Grant Agreement No. 159897 and 178895.

References

1. F. Yang, F. Gyger, and L. Thévenaz, *arXiv* **1911.04430** (2019).
2. G. Antonopoulos, et al, *Optics Express* **14**, 3000–3006 (2006).
3. CO_2 phase diagram data was obtained from: <https://encyclopedia.airliquide.com/carbon-dioxide>.
4. X. Liu, et al, *Optics Letters* **42**, 863–866 (2017).